Title

Cessation of berry growth coincides with leaf complete stomatal closure at pre-veraison for grapevine (Vitis vinifera) subjected to progressive drought stress.

Journal

Annals of Botany, 132(5)

Authors

Knipfer, T

Wilson, N

Jorgensen-Bambach, N

et al.

Publication Date

2023-11-30

DOI

10.1093/aob/mcad144

Peer reviewed

Annals of Botany **132**: 979–988, 2023
https://doi.org/10.1093/aob/mcad144, available online at www.academic.oup.com/aob

ANNALS OF BOTANY
Founded 1887

Cessation of berry growth coincides with leaf complete stomatal closure at pre-veraison for grapevine (*Vitis vinifera*) subjected to progressive drought stress

T. Knipfer[1,2,*], N. Wilson[1,2], N. E. Jorgensen-Bambach[3], A. J. McElrone[3,4], M. K. Bartlett[3] and S. D. Castellarin[1,2]

[1]Faculty of Land and Food Systems, The University of British Columbia, Vancouver, British Columbia V6T 1Z4, Canada, [2]Wine Research Centre, The University of British Columbia, Vancouver, British Columbia V6T 1Z4, Canada, [3]Department of Viticulture & Enology, University of California, Davis, CA 95616, USA, and [4]USDA-ARS, Crops Pathology and Genetics Research Unit, Davis, CA 95616, USA
[*]For correspondence. E-mail thorsten.knipfer@ubc.ca

Received: 25 March 2023 Returned for revision: 4 August 2023 Editorial decision: 11 September 2023 Accepted: 21 September 2023

• **Background and Aims** Drought events have devasting impacts on grape berry production. The aim of this study was to investigate berry growth in the context of leaf stomatal closure under progressive drought stress.
• **Methods** Potted grapevine plants (varieties 'Syrah' and 'Cabernet Sauvignon') were evaluated at pre-verasion (30–45 d after anthesis, DAA) and post-veraison (90–107 DAA). Berry diameter, berry absolute growth rate (AGR), leaf stomatal conductance (G_s) at midday, plant water potential at predawn and midday (Ψ_{PD} and Ψ_{MD}, respectively), and soil relative water content were measured repeatedly. The Ψ_{PD}-threshold of 90 % loss in stomatal conductance (G_{s10}, i.e. complete stomatal closure) was determined. Data were related to plant dehydration phases I, II and III with corresponding boundaries Θ_1 and Θ_2, using the water potential curve method.
• **Key Results** At pre-veraison, berry AGR declined together with leaf G_s in response to soil drying in both varieties. Berry AGR transitioned from positive to negative (shrinkage) values when leaf G_s approached zero. The G_{s10}-threshold was –0.81 MPa in 'Syrah' and –0.74 MPa in 'Cabernet Sauvignon' and was linked to boundary Θ_1. At post-veraison, berry AGR was negligible and negative AGR values were not intensified by increasing drought stress in either variety.
• **Conclusion** Leaf complete stomatal closure under progressive drought stress coincides with cessation of berry growth followed by shrinkage at pre-veraison (growth stage 1).

Key words: Development, plant–water relations, ripening, stomatal behaviour, stress thresholds.

INTRODUCTION

Climate change has accelerated the frequency and intensity of drought events worldwide with devastating impacts on agricultural and natural ecosystems (Gornall *et al.*, 2010; Choat *et al.*, 2018). Plant water stress by drought originates from insufficient soil water availability causing a water imbalance at the cell and organ level (Hsiao, 1973; Kramer and Boyer, 1995). Under drought conditions, leaf stomata closure is a key mechanism to limit water loss by transpiration while plant internal water resources are prioritized to developing reproductive organs (Gambetta *et al.*, 2020; Dietz *et al.* 2021; Harrison Day *et al.*, 2021). For grapevine, daily berry growth is dependent on net water accumulation (Matthews and Shackel, 2005). This requires that daily (night and day) water inflow from parent plant to berry exceeds daily water outflow (xylem backflow and berry transpiration) (Greenspan *et al.*, 1994, 1996). Hence, berry growth ceases and berries start to shrink due to excessive berry transpiration and/or xylem backflow (Zhang and Keller, 2015). Excessive xylem backflow is mainly linked to conditions of water stress by drought when the water potential (Ψ) of the parent plant becomes much more negative than that of the berry. Berries are particularly sensitive to drought-induced xylem backflows prior to ripening (i.e. at pre-veraison) when berry xylem is well connected to the xylem hydraulic system of the parent plant and berry sugar concentrations are relatively low (Greenspan *et al.*, 1994; Keller *et al.*, 2006; Knipfer *et al.*, 2015). However, it remains elusive how the cessation of berry growth (i.e. onset of shrinkage) is linked to leaf stomatal closure under progressive water stress by drought.

Frequency, length, severity and phenological timing of drought events can have various impacts on berry growth and development (e.g. Castellarin *et al.*, 2007; Gambetta *et al.*, 2020; Rienth *et al.*, 2021). Beneficial trade-offs between fruit quality, growth and soil water availability may be achieved under conditions of controlled water deficit, but this requires a comprehensive understanding of the coordination of physiological processes at the plant and berry level. Process-specific Ψ-thresholds provide important targets for water-deficit treatments and improved irrigation management (Gambetta *et al.*, 2020). Plant Ψ measured on an equilibrated leaf is directly related to the negative pressure that develops in xylem liquid under conditions of transpiration and/or soil drying (Scholander *et al.*, 1965; Turner and Long, 1980;

Turner, 1981). Considering a hydraulic continuum between plant and soil, plant Ψ measured at predawn (Ψ_{PD}) – when transpiration is negligible – serves as a useful surrogate for soil Ψ (Jones, 2007). For a given soil Ψ, differences in plant Ψ_{PD} and Ψ at midday (Ψ_{MD}) are mainly caused by changes in transpiration rates in response to atmospheric demand and leaf stomatal opening/closing (Martinez-Vilalta *et al.*, 2014; Charrier, 2020). For woody perennial crops facing drought stress, Knipfer *et al.* (2020*a*) showed that the Ψ-threshold of leaf complete stomatal closure can be predicted from the relationship between Ψ_{PD} and Ψ_{MD} by using a piecewise linear regression model (PLR) - the 'water potential (WP) curve'. The WP curve classifies plant dehydration into three phases and determines the boundaries that separate dehydration phases I and II (boundary Θ_1 'complete stomatal closure') and II and III (boundary Θ_2 'turgor loss point') (Fig. 1). However, it remains to be shown which dehydration phase is associated with cessation of berry growth and shrinkage in response to progressive drought stress (Fig. 1).

Greenspan *et al.* (1994, 1996) evaluated the diurnal water budget of the grape berry at pre- and post-verasion according to measured patterns of diurnal berry expansion/shrinkage and quantified the corresponding water flows across xylem, phloem and skin (transpiration). Here, we extend on the authors findings and provide specific insights into the coordination of leaf stomatal closure and cessation of berry growth under drought stress. Our hypothesis was that leaf complete stomatal closure delays the onset of berry shrinkage under progressive drought stress at pre-veraison by restricting excessive transpirational water loss from the parent plant, in turn allowing for prolonged berry water accumulation when soil water availability becomes limiting (Fig. 1). We studied varieties 'Syrah' and 'Cabernet Sauvignon' because of existing information on the hydraulic connection between parent plant and berry. For 'Syrah', berry shrinkage at post-veraison seems to be linked to xylem backflow late into fruit ripening (118 d after anthesis, DAA; Tilbrook and Tyerman, 2099). For 'Cabernet Sauvignon', xylem occlusions form in the pedicel at post-veraison but a hydraulic pathway of reduced conductivity appears to remain active (Knipfer *et al.*, 2015). We believe that the physiological data presented here may have future implications for developing irrigation management strategies that mitigate the risk of drought-induced berry shrinkage through knowledge about leaf stomatal thresholds.

MATERIALS AND METHODS

Plant growth

Own rooted 1.5-year-old plants (*Vitis vinifera* 'Syrah' and 'Cabernet Sauvignon', $n = 16$ plants per variety) were grown in 11.3-L pots filled with perennial soil mix (1:5 parts of peat moss, bark, compost, sand and perlite) in a glasshouse at the University of British Columbia, Vancouver campus. Plants were pruned to have two shoots that were bearing fruit clusters (n = 4-5 clusters per plant with on average 29 berries per cluster, and ~60 leaves per plant). Each shoot was trained to grow vertically along a stake; secondary shoots were removed prior to the experiment. Plants were maintained well-watered until the start of the experiment by hand-watering every 2–3 d with water containing a mix of nutrients. At 30 DAA (pre-veraison) and 90 DAA (post-veraison), a subset of $n = 8$ plants were randomly selected per variety and subjected to a 15–17-d experimental trial ($n = 4$ plants 'drydown' by not watering and $n = 4$ plants 'well-watered'). Using a digital balance, total pot weight (m_{Total}) was measured daily between 1900 and 2100 h for all plants, and m_{Total} of 'well-watered' plants was adjusted by adding the appropriate water weight using a graduated cylinder (1 mL H_2O = 1 g) (for details see next paragraph). For 'drydown' plants, day 1 was the first day plants were no longer watered (see Fig. 3 and Fig. 6). During the experiment trail, midday vapour pressure deficit (VPD) ranged from 1.6 to 3.2 kPa at pre-veraison (average day/night temperature of 27/20 °C and relative humidity of 55/73 %) and 0.9 to 2.5 kPa at post-veraison (average day/night temperature of 23/18 °C and relative humidity of 61/79 %); variations in VPD were due to changes in atmospheric conditions outside the glasshouse caused by sunny, cloudy or rainy days.

Bulk soil relative water content (soil RWC) was estimated according to $[(m_{H2O}/m_{H2O^*}) \times 100\ \%]$ where m_{H2O} = water weight and m_{H2O^*} = water weight at field capacity (Knipfer *et al.*, 2020*b*). The value of m_{H2O} was calculated according to $(m_{Total} - a - b - c)$ for parameters a = weight of plastic pot (=150 g), b = plant weight (=500 g on average) and c = soil dry weight. We determined that for a range in plant weight from 250 to 750 g calculated soil RWC only changed by 2–4 % which justified treating b as a constant (Supplementary Data Fig. S1). Soil dry weight (c) was determined according to $[(e - a - b) \times (1 - d)]$ for $e = m_{Total}$ at field capacity and d = fraction of soil water at field capacity [=0.74 of water weight/(water weight + dry weight)]. Parameter m_{H2O^*} (f) was calculated according to $[(e - a - b) \times d]$. Parameters a to f were treated as constants (Knipfer *et al.*, 2020*b*).

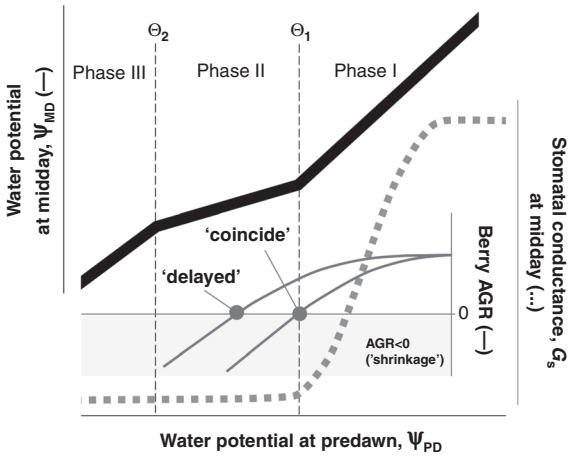

FIG. 1. Scheme illustrating the three plant dehydration phases of the WP curve with corresponding boundaries Θ_1 and Θ_2 for a grapevine subjected to drought stress. In addition, drought-induced reductions in midday leaf stomatal conductance are shown. This is complemented with two possible scenarios in drought-induced changes in absolute berry growth rates (AGR), i.e. cessation of berry growth (at AGR = 0) either 'coincides' with leaf complete stomatal closure (negligible G_s and Θ_1) or is 'delayed'.

Plant water potential

A Scholander-type pressure chamber (PMS Instrument Company, Model 615, Albany, OR, USA) was used to measure plant water potential at predawn (Ψ_{PD}) and at midday (Ψ_{MD}) every 1–2 d during the pre- and post-veraison experiment. On the evening prior to measurements (between 1900 and 2100 h), two mature and fully developed leaves (in close proximity to each other and located halfway along the same shoot) were covered with aluminium foil and a plastic bag to inhibit transpiration and allow for equilibration with stem xylem; shoots per plant were alternated to not defoliate one shoot over the course of the experiment. Subsequently, a dark plastic cover was pulled over the entire bench to minimize effects of nighttime canpoy transpiration and eliminate any light exposure that may trigger stomatal opening prior to measurement of Ψ_{PD} (Donovan *et al.*, 2001). The next morning at predawn (between 0500 and 0600 h), the canopy cover was pulled back, one bagged leaf per plant was excised, the bagged leaf was inserted in a second plastic bag and placed in a cooler. After completion of leaf sampling from all plants (<10 min), an excised and bagged leaf was placed in the pressure chamber with the petiole end protruding through chamber lid. The pressure in the chamber was raised slowly at a constant rate (about 0.01 MPa s^{-1}), and the balancing pressure (defined as plant Ψ) was recorded when a water meniscus started to form on the cut petiole surface. Following the same procedure, Ψ_{MD} was measured for the second bagged leaf that was still on the plant at midday (between 1200 and 1300 h).

The WP curve was defined as the relationship between Ψ_{PD} (*x*-axis) and Ψ_{MD} (*y*-axis). Plant dehydration phases I to III and corresponding boundaries Θ_1 and Θ_2 were determined using piecewise linear regression (PLR) models (Ryan and Porth, 2007; Knipfer *et al.*, 2020*a*). (Step-1) Datapoints were subjected to a triphasic PLR model. If the model predicted a significant ($P < 0.05$) boundary Θ_1 and Θ_2, and with all other model output parameters at $P < 0.05$, the model was accepted. To validate if the triphasic PLR model compared to a simple linear model provided a better fit, AICc (i.e. Akaike Information Criterion determined with AIC sample-size-adjusted formula) values were determined and the PLR model was used if the AICc value was lower by at least 2 points (Supplementary Data Table S1) (Burnham *et al.*, 2011). (Step-2) If the triphasic model only predicted one significant boundary value, datapoints were subjected to a biphasic PLR model. If the biphasic model predicted a significant ($P < 0.05$) boundary Θ_1, and with all other model parameters at $P < 0.05$, the model was accepted. Similar to Step-1, to validate if the biphasic PLR model compared to a simple linear model provided a better fit, AICc values were determined and the PLR model was used if the AICc value was lower by at least 2 points (Table S1). (Step-3) If no significant boundaries were detected using a triphasic or biphasic PLR model, datapoints were subjected to a simple linear 'monophasic' model.

Leaf stomatal conductance

Leaf stomatal conductance (G_s) was measured daily on a mature and completely developed leaf that was located on the same shoot and in between the two leaves used for Ψ_{PD} and Ψ_{MD}. Since leaves for Ψ measurements were bagged the previous evening, we were not able to take G_s and Ψ measurements on the same leaf. Measurements of G_s were taken at midday (between 1200 and 1300 h) using a LICOR-6400 gas exchange system. The leaf chamber was clamped to the leaf lamina about halfway between the leaf edge and initiation point of the petiole (CO_2 reference at 420 ppm, chamber block temperature at 25 °C, humidity at ~30 %; flow at 400 µmol s^{-1} and light intensity at 1500 µmol m^{-2} s^{-1}). To identify the best model fit of the relationship of midday G_s and Ψ_{PD}, all datapoints (variety, treatments, developmental stages) were pooled first (Table S2). The regression model that produced the lowest AICc value with all parameters significant ($P < 0.05$) was a sigmoidal three-parameter model; AICc value differences of at least 2 points were considered to identify the most strongly supported model (Burnham *et al.*, 2011). Subsequently, the Ψ_{PD} threshold was calculated at 90 % loss of maximum stomatal conductance (G_{s10}) and defined as 'leaf complete stomatal closure'; residual G_s was most likely due to cuticular transpiration.

Berry diameter and growth rate

Berry diameter was measured with a digital handheld caliper (between 1000 and 1100 h); berries measured were relatively loose and not tightly packed in the cluster. Great care was taken when placing the caliper to the widest diameter along the main berry axis to not squeeze the berry during measurement (i.e. especially at post-veraison when berries became soft); otherwise, the measurement and berry were discarded. For each plant, three to six berries (one to three per cluster) were tagged, measured every 2–3 d, and the average berry diameter ($Ø_{Berry}$) was determined. Berry absolute growth rate (AGR, in mm d^{-1}) was calculated as the difference in $Ø_{Berry}$ divided by the number of days between measurements. Values of berry AGR > 0 and AGR < 0 infered daily berry 'expansion' and 'shrinkage', respectively.

Data analysis

Linear and non-linear regression analyses were performed using SigmaPlot (version 14.5, Systat Software Inc., San Jose, CA, USA). A Student's t-test was used to identify statistically significant differences (at $P < 0.05$) between mean values.

RESULTS

Berry growth pattern

Berry growth followed a double sigmoidal pattern in well-watered plants of 'Syrah' and 'Cabernet Sauvignon' (Fig. 2A). The boundaries between growth stages were approximately at 45 and 59 DAA. Berry AGR declined during stage 1 from 0.35 to 0.09 mm d^{-1} in 'Syrah' and from 0.42 to 0.04 mm d^{-1} in 'Cabernet Sauvignon' (Fig. 2B). During stage 2, berry AGR continued to decline and reached ~0 mm d^{-1} at 59 DAA in both varieties (Fig. 2B). Berry AGR increased again at the beginning of stage 3 reaching a maximum at 76 DAA in 'Syrah' (0.23 mm d^{-1}) and 73 DAA in 'Cabernet Sauvignon' (0.14 mm d^{-1}).

Thereafter, berry AGR declined again and started to exhibit negative values in both varieties.

Pre-veraison

At 30–45 DAA, cessation of berry growth coincided with leaf complete stomatal closure in both varieties (Fig. 3). During the drydown, the decline in soil RWC resulted in a progressive reduction in Ψ_{PD} from ~ −0.5 MPa (day 1) to −2.0 MPa (day 15) in 'Syrah' and ~ −0.5 MPa (day 1) to −1.8 MPa (day 15) in 'Cabernet Sauvignon' (Fig. 3A–D). Berry AGR decreased from 0.4 mm d^{-1} in 'Syrah' and 0.2 mm d^{-1} in 'Cabernet Sauvignon' (day 1) to -0.1 mm d^{-1} (i.e. daily shrinkage) in both varieties (day 6) (Fig. 3E, F). This corresponded to a Ψ_{PD} of −0.8 MPa in 'Syrah' and –0.6 MPa in 'Cabernet Sauvignon' (day 6) (Fig. 3C, D). Leaf midday G_s dropped from ~0.2 mol s^{-1} m^{-2} in 'Syrah' and ~0.25 mol s^{-1} m^{-2} in 'Cabernet Sauvignon' (day 1) to 0.017 mol s^{-1} m^{-2} in 'Syrah' and 0.034 mol s^{-1} m^{-2} in 'Cabernet Sauvignon' (day 6) (Fig. 3G, H).

The relationship of leaf midday G_s and berry AGR indicated that berry AGR of ≤0 mm d^{-1} coincided with G_s of ≤0.022 mol s^{-1} m^{-2} in 'Syrah' and ≤0.034 mol s^{-1} m^{-2} in 'Cabernet Sauvignon (Fig. 4). On the other hand, berry AGR was positive and fairly steady when G_s was >0.16 mol s^{-1} m^{-2} for 'Syrah' (Fig. 4A) and >0.20 mol s^{-1} m^{-2} for 'Cabernet Sauvignon' (Fig. 4B).

The Ψ_{PD} threshold of G_{s10} was detected in plant dehydration phase I and was associated with boundary Θ_1 in both varieties (Fig. 5). Maximum midday G_s (as predicted by the fitted sigmoidal curve) was 0.19 mol s^{-1} m^{-2} for 'Syrah' and 0.30 mol s^{-1} m^{-2} for 'Cabernet Sauvignon' (Fig. 5A, B; see also Supplementary Data Table S3). The threshold of G_{s10} was at −0.81 MPa in 'Syrah' and −0.74 MPa in 'Cabernet Sauvignon' (Fig. 5A, B), which corresponded to a midday G_s of 0.019 and 0.030 mol s^{-1} m^{-2}, respectively. For both varieties, these midday G_s values were associated with the onset of berry 'shrinkage' (see Fig. 3 on day 6; Fig. 4). For 'Syrah', the WP curve was triphasic with a boundary Θ_1 and Θ_2 at −0.98 and −1.24 MPa, respectively (Fig. 5C; see also Table S4). For 'Cabernet Sauvignon', the WP curve was biphasic with a boundary Θ_1 at −0.80 MPa (Fig. 5D; Table S4). The difference in Ψ_{PD} between G_{s10} and Θ_1 was 0.06 MPa for 'Cabernet Sauvignon and 0.17 MPa for 'Syrah' (Fig. 5).

Post-veraison

At 90–107 DAA, berry growth was negligible for 'well-watered' and 'drydown' plants in both varieties (Fig. 6; see also Fig. 2). During the drydown, the decline in soil RWC was associated with a reduction in Ψ_{PD} from –0.3 to –2.3 MPa in 'Syrah' and ~ −0.3 to −2.0 MPa in 'Cabernet Sauvignon' (Fig. 6A–D). For both varieties, berry AGR was close to zero and most often negative under well-watered and drydown conditions throughout the experiment (Fig. 6E). For 'Cabernet Sauvignon', a similar pattern was observed; there was no consistent change in berry AGR in response to a decline in Ψ_{PD}. Leaf midday G_s ranged initially between 0.245–0.3 mol s^{-1} m^{-2} in both varieties and declined over the course of the drydown reaching a value of 0.041 mol s^{-1} m^{-2} in 'Syrah' and 0.037 mol s^{-1} m^{-2} in 'Cabernet Sauvignon' (day 8) (Fig. 6G, H).

Threshold of G_{s10} was detected during plant dehydration phase I for both varieties (Fig. 7). Maximum G_s at midday was 0.17 mol s^{-1} m^{-2} for 'Syrah' and 0.22 mol s^{-1} m^{-2} for 'Cabernet Sauvignon' as predicted by the fitted sigmoidal curve (Fig. 7A, B; see also Supplementary Data Table S3). Subsequently, G_{s10} was calculated at –0.61 MPa in 'Syrah' and –0.64 MPa in 'Cabernet Sauvignon' that corresponded to a midday G_s of 0.017 and 0.022 mol s^{-1} m^{-2}, respectively (Fig. 7A, B; see also Table S3). For 'Syrah', the WP curve was triphasic with a boundary Θ_1 and Θ_2 at −1.11 and −1.80 MPa, respectively (Fig. 7C; see Table S4). For 'Cabernet Sauvignon', the WP curve was also triphasic with a boundary Θ_1 at −0.78 MPa and Θ_2 at −1.51 MPa. respectively (Fig. 7D; Table S4). The difference in Ψ_{PD} between G_{s10} and Θ_1 was 0.13 MPa for 'Cabernet Sauvignon' and 0.5 MPa for 'Syrah'. In both varieties the difference between G_{s10} and boundary Θ_2 was more than 0.8 MPa (Fig. 7).

DISCUSSION

In this study on grapevine (varieties 'Syrah' and 'Cabernet Sauvignon') subjected to progressive drought stress, we found

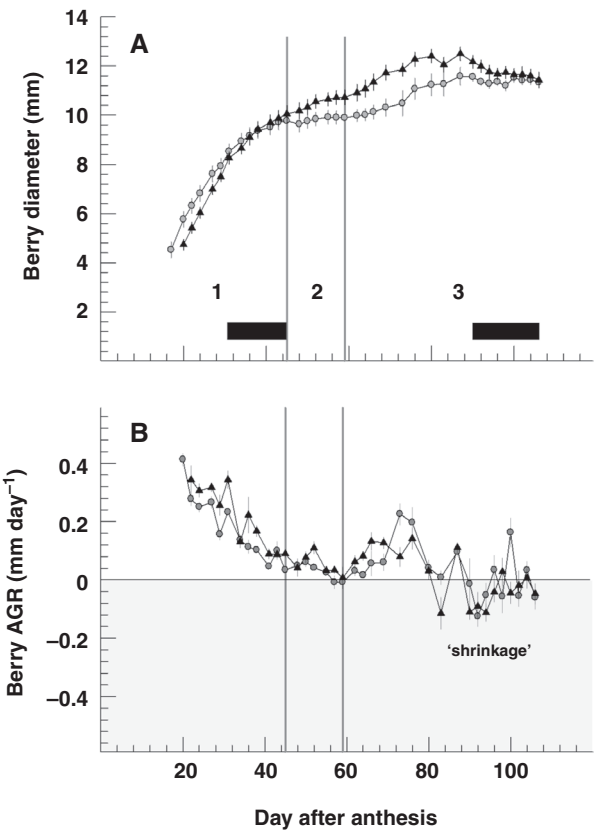

FIG. 2. Berry growth dynamics of grapevine variety 'Syrah' (triangles) and 'Cabernet Sauvignon' (circles) under well-watered conditions. The black boxes indicate the experimental time periods at pre-veraison (30–45 d after anthesis, DAA) and post-veraison (90–107 DAA). (B) Berry absolute growth rate (AGR) over days after anthesis. The shaded area indicates berry shrinkage at AGR < 0. Each data point in A and B is the mean ± s.e. of $n = 4$ plants. Vertical lines are the estimated boundaries between berry growth stages 1 to 3.

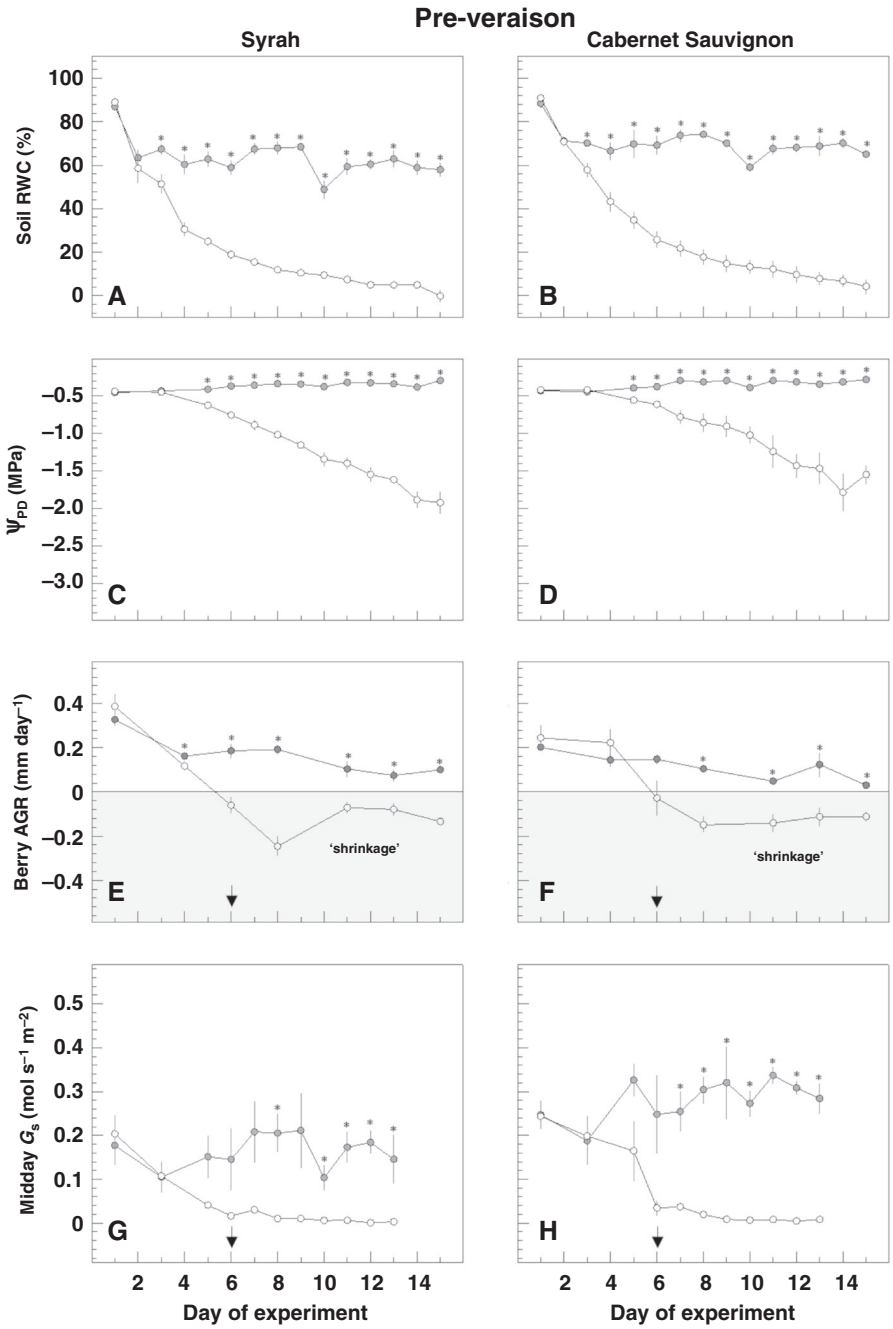

FIG. 3. Temporal changes in soil relative water content (A, B), plant water potential at predawn (C, D), berry absolute growth rate (E, F) and leaf stomatal conductance at midday (G, H) under well-watered (solid symbols) and progressive drought (open symbols) conditions at pre-veraison. (E, F) The shaded area indicates berry shrinkage at AGR < 0. (E–H) The arrow indicates the first day berry AGR was <0. (A–H) Each data point is the mean ± s.e. of $n = 4$ plants. For a given day, an asterisk indicates a statistically significant difference (at $P < 0.05$) between means of 'well-watered' and 'drydown' plants.

that leaf complete stomatal closure (defined at G_{s10}) coincides with cessation in berry growth at pre-veraison (30–45 DAA, stage 1). Between varieties G_{s10} occurred at a comparable Ψ_{PD} of –0.81 MPa in 'Syrah' and –0.74 MPa in 'Cabernet Sauvignon' (i.e. only <0.1 MPa difference) and was detected towards the end of plant dehydration phase I as determined with the WP curve. We speculate that negative berry AGR (i.e. shrinkage) during plant dehydration phases II and III, and as observed from day 6 to 14 when midday G_s was negligible, was linked to excessive xylem backflow that could not be compensated for by sufficient water inflow via xylem and phloem in both varieties (see Greenspan *et al.*, 1994). Rates of berry shrinkage were comparable (i.e. around –0.1 to –0.2 mm d^{-1}) between varieties. Together, drought-induced reductions in leaf midday G_s can slow down the decline in Ψ_{PD} over time by reducing transpirational water loss but the onset of berry shrinkage (AGR < 0) is not delayed by leaf complete stomatal closure (see Fig. 3).

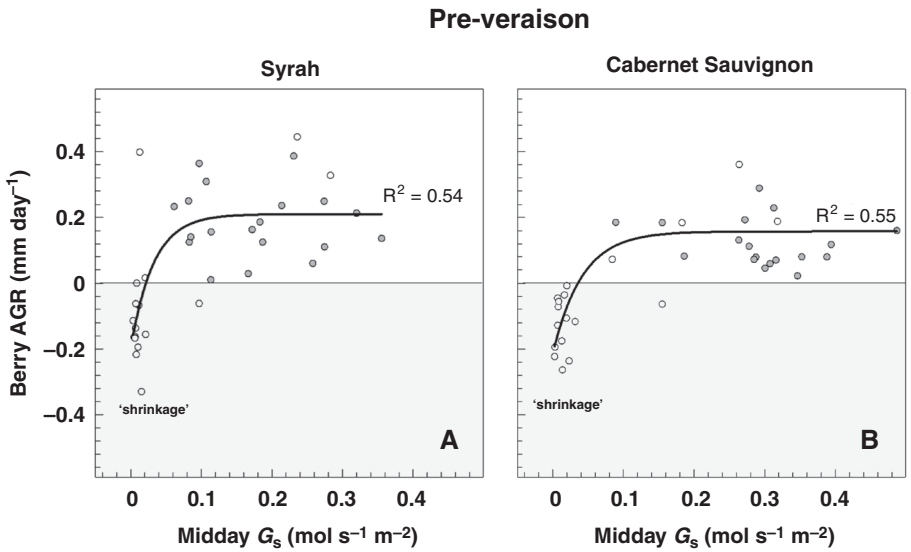

FIG. 4. Relationship of leaf stomatal conductance at midday and berry absolute growth rate (corresponding to Fig. 3). Symbols correspond to grapevines under well-watered (solid symbols) or progressive drought (open symbols) conditions. Each symbol represents a measurement of an individual plant. The shaded area indicates berry shrinkage at AGR < 0. The solid line is a non-linear regression (exponential rise to maximum, $P < 0.0001$) that best described the pattern of data points.

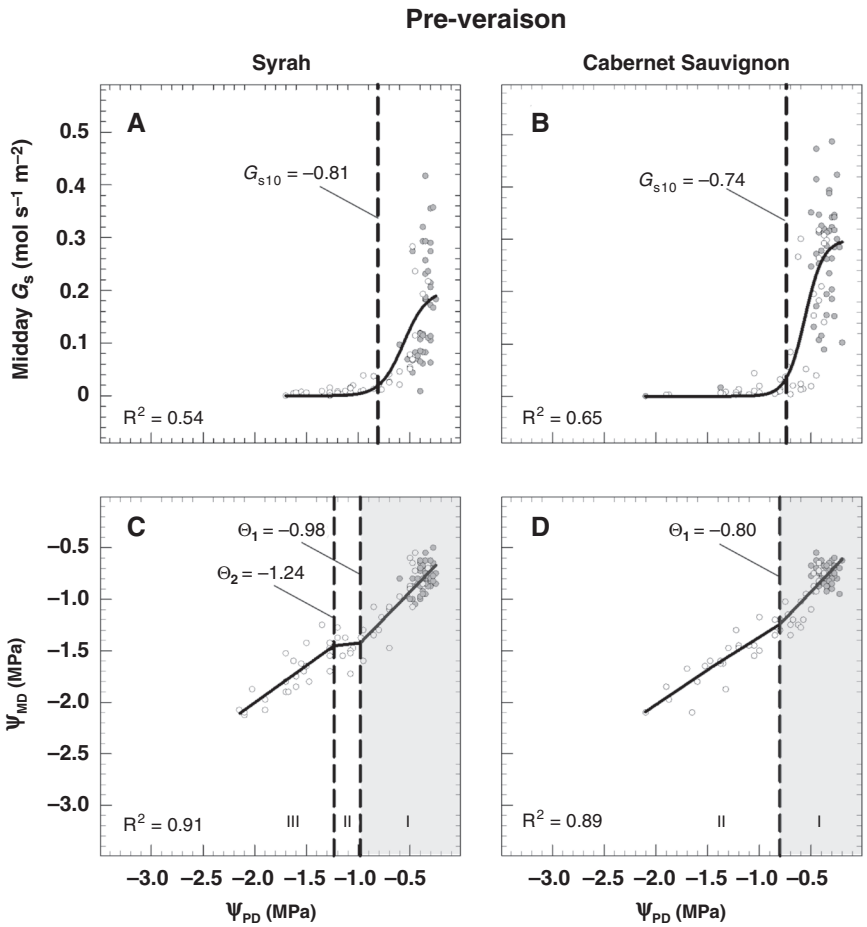

FIG. 5. (A, B) Relationship of leaf stomatal conductance at midday and plant water potential at predawn for grapevines at pre-veraison. Solid lines are non-linear regressions (sigmoidal three-parameter, $P < 0.0001$). Vertical lines indicate G_{s10} (i.e. 90 % loss in G_s). (C, D) Corresponding WP curves established from the relationship of plant water potential at predawn and midday. Roman numerals indicate plant dehydration phases I–III. The shaded area highlights phase I. Vertical lines are boundaries Θ_1 and Θ_2. Solid lines are piecewise linear regressions ($P < 0.0001$). (A–D) Each data point is a measurement of an individual plant.

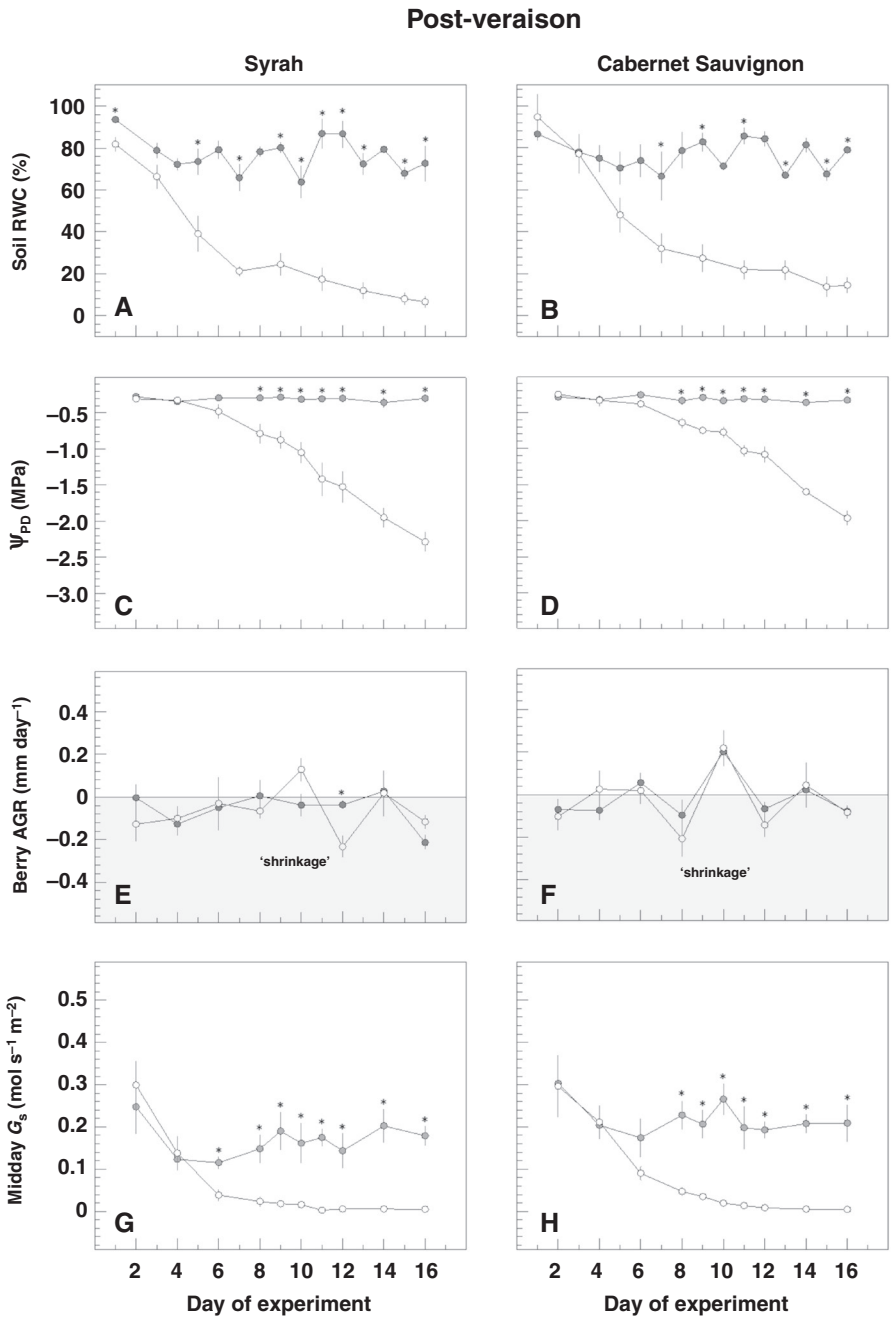

FIG. 6. Temporal changes in soil relative water content (A, B), plant water potential at predawn (C, D), berry absolute growth rate (E, F) and leaf stomatal conductance at midday (G, H) under well-watered (solid symbols) and progressive drought (open symbols) conditions at post-veraison. (E, F) The shaded area indicates berry shrinkage at AGR < 0. (A–H) Each data point is the mean ± s.e. of $n = 4$ plants. For a given day, an asterisk indicates a statistically significant difference (at $P < 0.05$) between means of 'well-watered' and 'drydown' plants.

At post-verasion, berry shrinkage occured under 'well-watered' and 'drydown' conditions in 'Syrah' and 'Cabernet Sauvignon', and the rate of berry shrinkage was comparable between varieties under both conditions. Hence, berry shrinkage between 90 and 107 DAA could not be attributed to limited soil water availability. The fact that negative berry AGR did not intensify under progressive drought stress (i.e. decline in Ψ_{PD}) was probably due to the presence of xylem occlusions limiting xylem backflow from berry to parent plant and/or a relatively low berry Ψ due to sugar accumulation at post-veraison (Keller *et al.*, 2006, 2015; Wada *et al.*, 2008; Choat *et al.*, 2009; Knipfer *et al.*, 2015). Carlomagno *et al.* (2018) showed that xylem backflow is active in pre- but not post-verasion berries of 'Syrah' using acid fuchsin as xylem tracer. Xylem occlusions were detected in vessels of the berry pedicel in 'Cabernet Sauvignon' at post-veraison (Knipfer *et al.*, 2015). However, if we assume that a residual hydraulic pathway of reduced conductivity remained active

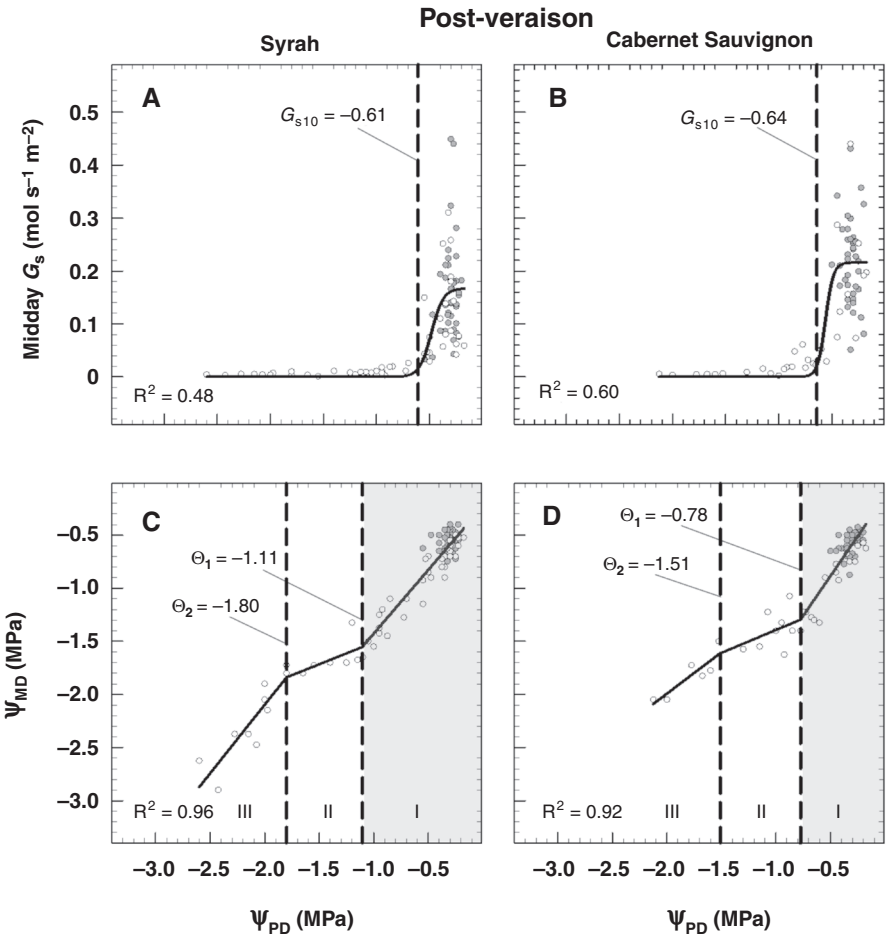

FIG. 7. (A, B) Relationship of leaf stomatal conductance at midday and plant water potential at predawn for grapevines at post-veraison. Solid lines are non-linear regressions (sigmoidal three-parameter, $P < 0.0001$). Vertical lines indicate G_{s10} (i.e. 90 % loss in G_s). (C, D) Corresponding WP curves established from the relationship of plant water potential at predawn and midday. Roman numerals indicate plant dehydration phases I–III. The shaded area highlights phase I. Vertical lines are boundaries Θ_1 and Θ_2. Solid lines are piecewise linear regressions ($P < 0.0001$). (A–D) Each data point is a measurement of an individual plant.

(see Tilbrook and Tyerman, 2009), leaf complete stomatal closure may have helped to prevent more intensive berry shrinkage by restricting transpirational water loss and reducing rates of xylem backflow; this may also have been the case at pre-veraison where rates of berry shrinkage (i.e. AGR < 0) remained fairly constant after leaf complete stomatal closure. Previously, berry shrinkage at post-veraison has been reported to be more pronounced in 'Syrah' than in other varieties (e.g. Tilbrook and Tyerman, 2009) under well-watered conditions, but our data provide no clear evidence that berry AGR is more negative in 'Syrah' compared to 'Cabernet Sauvignon' under well-watered conditions. Day 16 of the drydown may suggest this, when the rate of shrinkage was around −0.2 mm d^{-1} in 'Syrah' and only −0.04 mm d^{-1} in 'Cabernet Sauvignon', but this also corresponded to a lower Ψ_{PD} in 'Syrah' (−2.3 MPa) compared to 'Cabernet Sauvignon' (−2.0 MPa) on that day. In summary, our data are in support of previous findings that water stress by drought has rather negligible effects on berry shrinkage at post-veraison even if some hydraulic connection remains between berry and parent plant (Greenspan *et al.*, 1994, 1996; Keller *et al.*, 2006; and as cited above).

The thresholds of G_{s10} occurred towards the end of plant dehydration phase I of the WP curve, and was comparable to boundary Θ_1 for 'Syrah' (at pre-veraison) and 'Cabernet Sauvignon' (at pre- and post-veraison). In contrast, Charrier (2020) suggested that leaf stomatal closure is rather linked to boundary Θ_2 in grapevine. However, based on data by Knipfer *et al.* (2020*a*) on walnut, Θ_2 is linked to the turgor loss point (Ψ_{TLP}). Leaf pressure–volume curves allow to determine Ψ_{TLP} (Kramer and Boyer, 1995; Sack and Pasquet-Kok, 2010; Bartlett *et al.*, 2012, 2021). Dayer *et al.* (2020) found a Ψ_{TLP} of −1.5 MPa for 'Syrah', which is only slightly more negative than our Θ_2 of −1.2 MPa at pre-veraison. Moreover, Alsina *et al.* (2007) found a reduction in Ψ_{TLP} from fruit set to harvest in several grape varieties. Similarily, our Θ_2 dropped to more negative values from pre- to post-veraison (i.e. from −1.2 to −1.8MPa) in 'Syrah'. Nevertheless, we did not detect a boundary Θ_2 at pre-veraison for 'Cabernet Sauvignon'. We speculate that the reason for this observation is that both G_{s10} and Ψ_{TLP} coincided in this variety at pre- but not post-veraison.

For our fruit-bearing plants, G_{s10} was more negative at pre- compared to post-verasion (by 0.2 MPa in 'Syrah' and 0.1 MPa in 'Cabernet Sauvignon'). This indicates that stomata closed

'earlier' at post-veraison under increasing drought stress in both varieties. Since our post-veraison experiment was conducted late into berry development, we speculate that 'earlier' stomatal closure at less negative Ψ_{PD} was a response to limit transpirational water loss over maintaining CO_2 capture (photosynthesis); energy demands for berry growth/developmental are negligible at this point. In contrast, Herrera *et al.* (2022) reported that stomatal responses become increasingly more tolerant to more negative plant Ψ over the growing season, and complete stomata closure occurs at more negative plant Ψ. One reason for the difference in stomatal responses observed here and by Herrera *et al.* (2022) may be fruit load since the latter authors performed their study on plants that did not bear fruits. Effects related to plant development and growing conditions at the time of measurements may also contribute to this difference.

Plant Ψ measured at midday on an equilibrated leaf (stem water potential) responds to air VPD when the remaining leaves of the canopy are transpiring (stomata are open); that is so because transpiration rates impact xylem pressure (Shackel, 2011). Therefore, one may argue that the observed differences in WP curve characteristics from pre- to post-veraison are predominantly a VPD response. However, our data show that Ψ_{MD} responded similarly to VPD at pre- and post-verasion for both varieties (Supplementary Data Fig. S2). For 'Syrah', we determined a change in Ψ_{MD} of –0.09 MPa per 1-kPa change in air VPD at pre-veraison and –0.08 MPa kPa^{-1} at post-veraison (Fig. S2). Also, there was no significant difference in the response of Ψ_{MD} to VPD between pre-veraison (–0.07 MPa kPa^{-1}) and post-veraison (–0.06 MPa kPa^{-1}) for 'Cabernet Sauvignon' (Fig. S2). In addition, responses in midday G_s, and in turn G_{s10} values, were not dependent on air VPD conditions since midday G_s was measured on leaves clamped inside an environmentally controlled cuvette of the LICOR gas exchange system (Fig. S2).

The ability of plants to maintain xylem pressure under drought is typically described using the concept of isohydricity (Tardieu and Simonneau, 1998; Meinzer *et al.*, 2016; Martinez-Vilalta *et al.*, 2014; for A review see Hochberg *et al.*, 2018). Our WP curves suggest a shift towards a more isohydric behaviour (i.e. shallower slopes) in phase II of the WP curve at pre- and post-veraison in both varieties. In addition to stomatal closure at Θ_1, we speculate that stem water release into the transpiration stream (Holbrook 1995) and reduced root water loss to the drying soil environment (Cuneo *et al*, 2016, 2021) contributed to this shift from an aniso- (steeper slope, phase I) to isohydric (shallower slope, phase II) behaviour.

CONCLUSION

Over the last decades, grapevine water relations have been investigated to better understand the impact of soil water availability on berry growth (Matthews and Anderson, 1989; Greenspan *et al.*, 1994, 1996; Matthews and Shackel, 2005; Castellarin *et al.*, 2007, 2011; Wada *et al.*, 2008; Choat *et al.*, 2009; Shackel, 2011; Knipfer *et al.*, 2015; Gambetta *et al.*, 2020). Here, we show that cessation of berry growth coincides with leaf complete stomatal closure at pre-veraison (berry growth stage 1) for grapevine varieties 'Syrah' and 'Cabernet Sauvignon' subjected to progressive drought stress. However, this does not mean that there is a mechanistic link between both processes but rather highlights that both process-specific thresholds are associated with the same plant stress status. Since berry growth is maintained prior to reaching G_{s10}, G_{s10} (with respect to Ψ_{PD}) can be an important irrigation target that prevents cessation of berry growth when water resources are limited. Between the two varieties tested, our data indicate no major differences in the timing of cessation of berry growth under progressive drought and its relation to leaf complete stomata closure. Future studies may be directed towards resolving the recovery potential of berry growth rate following shrinkage.

SUPPLEMENTARY DATA

Supplementary data are available at *Annals of Botany* online and consist of the following.

Figure S1: Soil relative water content determined for different plant weights. Figure S2: Relationship of air vapour pressure deficit (VPD) versus plant water potential at midday or leaf stomatal conductance for grapevines under well-watered conditions. Table S1: Regression models (at $P < 0.05$) applied to the relationship of Ψ_{MD} (*y*-axis) and Ψ_{PD} (*x*-axis) corresponding to Figs 5 and 7. Table S2: Regression models (at $P < 0.05$) applied to the relationship of midday G_s (*y*-axis) and Ψ_{PD} (*x*-axis) for all datapoints between varieties, treatments and developmental stages. Table S3. Calculated values of midday G_{smax} and G_{s10} from non-linear sigmoidal regressions including 95 % confidence intervals and standard errors (corresponding to Figs 5 and 7). Table S4. Boundary values extracted from WP curves including 95 % confidence intervals and standard errors (corresponding to Figs 5 and 7).

AUTHOR CONTRIBUTIONS

T.K. designed and performed the experiments together with S.D.C., analysed the data, and wrote the article; N.W. helped with measurement of water potential, leaf gas exchange, and berry diameters and data analyses; N.B. helped in analyses of water potential curves, and revised the article; A.J.M. and M.K.B. revised the article; S.D.C. designed and performed experiments together with T.K., and revised the article. The authors have no conflicts of interest to declare.

FUNDING

This research was supported by operating grants from the Natural Sciences and Engineering Research Council of Canada (NSERC, GR019368 awarded to T.K. and NSERC GR000096 awarded to S.D.C.).

ACKNOWLEDGMENTS

We thank Gopal Sharma and Abel Rosado for help with plant maintenance and support of physiological measurements (both UBC Vancouver). We also thank Prof. Markus Keller (Washington State University, USA) and the anonymous reviewers for providing their valuable feedback and suggestions on an earlier version.

LITERATURE CITED

Alsina MM, **de Herralde F**, **Aranda X**, **Save R**, **Biel C. 2007**. Water relations and vulnerability to embolism are not related: Experiments with eight grapevine cultivars. *Vitis-Geilweilerhof* **46**: 1–7.

Bartlett MK, **Scoffoni C**, **Sack L. 2012**. The determinants of leaf turgor loss point and prediction of drought tolerance of species and biomes: a global meta-analysis. *Ecology Letters* **15**: 393–405. doi:10.1111/j.1461-0248.2012.01751.x.

Bartlett MK, **Sinclair G**, **Fontanesi G**, **Knipfer T**, **Walker MA**, **McElrone AJ. 2021**. Root pressure–volume curve traits capture rootstock drought tolerance. *Annals of Botany* **129**: 389–402. doi:10.1093/aob/mcab132.

Burnham KP, **Andrerson DR**, **Huyvaert KP. 2011**. AIC model selection and multimodel inference in behavioral ecology: some background, observations, and comparisons. *Behavioral Ecology and Sociobiology* **65**: 23–25.

Carlomagno A, **Novello V**, **Ferrandino A**, **Genre A**, **Lovisolo C**, **Hunter JJ. 2018**. Pre-harvest berry shrinkage in cv 'Shiraz' (*Vitis vinifera* L.): Understanding sap flow by means of tracing. *Scientia Horticulturae* **233**: 394–406. doi:10.1016/j.scienta.2018.02.014.

Castellarin SD, **Pfeifer A**, **Sililotti P**, **Degan M**, **Peterlunger E**, **Gaspero GD. 2007**. Transcriptional regulation of anthocyanin biosynthesis in ripening berries of grapevine under seasonal water deficit. *Plant, Cell and Environment* **30**: 1381–1399.

Castellarin SD, **Gambetta GA**, **Wada H**, **Shackel KA**, **Matthews MA. 2011**. Fruit ripening in *Vitis vinifera*: spatiotemporal relationships among turgor, sugar accumulation, and anthocyanin biosynthesis. *Journal of Experimental Botany* **62**: 4345–4354. doi:10.1093/jxb/err150.

Charrier G. 2020. Extrapolating physiological response to drought through step-by-step analysis of water potential. *Plant Physiology* **184**: 560–561. doi:10.1104/pp.20.01110.

Choat B, **Gambetta GA**, **Shackel KA**, **Matthews MA. 2009**. Vascular function in grape berries across development and its relevance to apparent hydraulic isolation. *Plant Physiology* **151**: 1677–1687. doi:10.1104/pp.109.143172.

Choat B, **Brodribb TJ**, **Brodersen CR**, **Duursma RA**, **Lopez R**, **Medlyn BE. 2018**. Triggers of tree mortality under drought. *Nature* **558**: 531–539. doi:10.1038/s41586-018-0240-x.

Cuneo IF, **Knipfer T**, **Brodersen CR**, **McElrone AJ. 2016**. Mechanical failure of fine root cortical cells initiates plant hydraulic decline during drought. *Plant Physiology* **172**: 1669–1678. doi:10.1104/pp.16.00923.

Cuneo IF, **Barrios-Masias F**, **Knipfer T**, ***et al***. **2021**. Differences in grapevine rootstock sensitivity and recovery from drought are linked to fine root cortical lacunae and root tip function. *The New Phytologist* **229**: 272–283. doi:10.1111/nph.16542.

Dayer S, **Herrera JS**, **Dai Z**, ***et al***. **2020**. The sequence and thresholds of leaf hydraulic traits underlying grapevine varietal differences in drought tolerance. *Journal of Experimental Botany* **71**: 4333–4344.

Dietz KJ, **Zoerb C**, **Geilfus CM. 2021**. Drought and crop yield. *Plant Biology* **23**: 881–893.

Donovan LA, **Linton MJ**, **Richards JH. 2001**. Predawn plant water potential does not necessarily equilibrate with soil water potential under well-watered conditions. *Oecologia* **129**: 328–335. doi:10.1007/s004420100738.

Gambetta GA, **Herrera JC**, **Dayer S**, **Feng Q**, **Hochberg U**, **Castellarin SD. 2020**. The physiology of drought stress in grapevine: towards an integrative definition of drought tolerance. *Journal of Experimental Botany* **71**: 4658–4676. doi:10.1093/jxb/eraa245.

Gornall J, **Betts R**, **Burke E**, ***et al***. **2010**. Implications of climate change for agricultural productivity in the early twenty-first century. *Philosophical Transactions of the Royal Society of London, Series B: Biological Sciences* **365**: 2973–2989. doi:10.1098/rstb.2010.0158.

Greenspan MD, **Shackel KA**, **Matthews MA. 1994**. Developmental changes in the diurnal water budget of the grape berry exposed to water deficit. *Plant Cell and Environment* **17**: 811–820. doi:10.1111/j.1365-3040.1994.tb00175.x.

Greenspan MD, **Schultz HR**, **Matthews MA. 1996**. Field evaluation of water transport in grape berries during water deficit. *Physiologia Plantarum* **97**: 55–62. doi:10.1034/j.1399-3054.1996.970109.x.

Harrison Day BL, **Carins-Murphy MR**, **Brodribb TJ. 2021**. Reproductive water supply is prioritized during drought in tomato. *Plant Cell and Environment* **45**: 69–79. doi:10.1111/pce.14206.

Herrera JC, **Calderan A**, **Gambetta GA**, ***et al***. **2022**. Stomatal responses in grapevine become increasingly more tolerant to low water potentials throughout the growing season. *The Plant Journal* **109**: 804–815. doi:10.1111/tpj.15591.

Hochberg U, **Rockwell FE**, **Holbrook MN**, **Cochard H. 2018**. Iso/anisohydry: a plant–environment interaction rather than a simple hydraulic trait. *Trend in Plant Science* **23**: 112–120.

Holbrook NM. 1995. Stem water storage. In **Gartner BL**, ed. *Plant stem: physiology and functional morphology*. San Diego: Academic Press, 151–169.

Hsiao TC. 1973. Plant responses to water stress. *Annual Review of Plant Physiology* **24**: 519–570.

Jones HG. 2007. Monitoring plant and soil water status: established and novel methods revisited and their relevance to studies of drought tolerance. *Journal of Experimental Botany* **58**: 119–130. doi:10.1093/jxb/erl118.

Keller M, **Smith JP**, **Bondada BR. 2006**. Ripening grape berries remain hydraulically connected to the shoot. *Journal of Experimental Botany* **57**: 2577–2587. doi:10.1093/jxb/erl020.

Keller M, **Zhang Y**, **Shrestha M**, **Biondi M**, **Bondada BR. 2015**. Sugar demand of ripening grape berries leads to recycling of surplus phloem water via the xylem. *Plant, Cell and Environment* **38**: 1048–1059.

Knipfer T, **Fei J**, **Gambetta GA**, **McElrone AJ**, **Shackel KA**, **Matthews MA. 2015**. Water transport properties of the grape pedicel during berry development: Insights into xylem anatomy and function using microtomography. *Plant Physiology* **168**: 1590–1602. doi:10.1104/pp.15.00031.

Knipfer T, **Bambach N**, **Hernandez MI**, ***et al***. **2020***a*. Predicting stomatal closure and turgor loss in woody plants using predawn and midday water potential. *Plant Physiology* **184**: 881–894. doi:10.1104/pp.20.00500.

Knipfer T, **Reyes C**, **Momayyezi M**, **Kluepfel D**, **McElrone AJ. 2020***b*. A comparative study on physiological responses of commercially available walnut genotypes (RX1, Vlach and VX211) to drought stress. *Trees* **34**: 665–678.

Kramer PJ, **Boyer JS. 1995**. *Water relations of plants and soils*. New York: Academic Press.

Martinez-Vilalta J, **Poyatos R**, **Retana AD**, **Mencuccini M. 2014**. A new look at water transport regulation in plant. *New Phytologist* **205**: 105–115.

Matthews MA, **Anderson MM. 1989**. Reproductive development in grape (*Vitis vinifera* L.): responses to seasonal water deficits. *American Journal of Enology and Viticulture* **40**: 52–60.

Matthews MA, **Shackel KA. 2005**. Growth and water transport in fleshy berry. In: **Holbrook NM**, **Zwieniecki MA**, eds. *Vascular transport in plants*. Burlington: Elsevier Academic Press.

Meinzer CF, **Woodruff DR**, **Marias DE**, ***et al***. **2016**. Mapping 'hydroscapes' along the iso- to anisohydric continuum of stomatal regulation of plant water status. *Ecology Letters* **19**: 1343–1352.

Rienth M, **Vigneron N**, **Darriet P**, ***et al***. **2021**. Grape berry secondary metabolites and their modulation by abiotic factors in a climate change scenario – a review. *Frontiers in Plant Science* **12**: 1–26.

Ryan SE and **Porth LS. 2007**. *A tutorial on the piecewise regression approach applied to bedload transport data*. General Technical Report RMRS-GTR-189. Fort Collins, CO: US Department of Agriculture, Forest Service, Rocky Mountain Research Station. 41.

Sack L, **Pasquet-Kok J. 2010**. Leaf pressure-volume curve parameters. *PrometheusWiki*. https://prometheusprotocols.net/function/water-relations/pressure-volume-curves/leaf-pressure-volume-curve-parameters/.

Scholander PF, **Bradstreet ED**, **Hemmigsen EA**, **Hammel HT. 1965**. Sap pressure in vascular plants. *Science* **148**: 339–346.

Shackel K. 2011. A plant-based approach to deficit irrigation in trees and vines. *HortScience* **46**: 173–177. doi:10.21273/hortsci.46.2.173.

Tardieu F, **Simonneau T. 1998**. Variability among species of stomatal control under fluctuating soil water status and evaporative demand: modelling isohydric and anisohydric behaviors. *Journal of Experimental Botany* **49**: 419–432.

Tilbrook J, **Tyerman SD. 2009**. Hydraulic connection of grape berries to the vine: varietal differences in water conductance into and out of berries, and potential for backflow. *Functional Plant Biology* **36**: 541–550. doi:10.1071/FP09019.

Turner NC. 1981. Techniques and experimental approaches for the measurement of plant water status. *Plant and Soil* **58**: 339–366. doi:10.1007/bf02180062.

Turner NC, **Long MJ. 1980**. Errors arising from rapid water loss in the measurement of leaf water potential by the pressure chamber technique. *Functional Plant Biology* **7**: 527–537. doi:10.1071/pp9800527.

Wada H, **Shackel KA**, **Matthews MA. 2008**. Berry ripening in *Vitis vinifera*: apoplastic solute accumulation accounts for pre-veraison turgor loss in berries. *Planta* **227**: 1351–1361. doi:10.1007/s00425-008-0707-3.

Zhang Y, **Keller M. 2015**. Grape berry transpiration is determined by vapor pressure deficit, cuticular conductance, and berry size. *American Journal of Enology and Viticulture* **66**: 454–462. doi:10.5344/ajev.2015.15038.